Experimental and theoretical investigation of three dimensional strain occurring near the surface in asphalt concrete layers

Damien Grellet, Guy Dore, Jean-Pierre Kerzreho, Jean-Michel Piau, Armelle Chabot, Pierre Hornych

Experimental and theoretical investigation of three dimensional strain occurring near the surface in asphalt concrete layers

Grellet Damien[1], Doré Guy[1], Kerzreho Jean-Pierre[2], Piau Jean-Michel[2], Chabot Armelle[2] and Hornych Pierre[2]

[1]Department of Civil Engineering, Laval University, Québec (QC), Canada
[2]L'UNAM Université, IFSTTAR, CS4, F-44344 BOUGUENAIS Cedex, France

Abstract. *Several pavement failures have been observed to be initiated at or near the surface of the hot-mix asphalt layers and some of them propagate downward through the surface layer (top-down cracking). These modes of failure are affected by heavy vehicular loading configuration, pavement structure and their interaction at the tire-pavement contact. This paper documents an experimental investigation of surface strain induced under the entire tire by using specific instruments based on fiber optic sensors. Two innovative retrofit techniques which allow measuring strains in the upper parts of the asphalt layer have been used on the IFSTTAR's test track facility. The association of these two techniques allows obtaining the strains, few centimeters below the surface, in three directions: longitudinal, transverse and vertical. Two pavement structures with two temperatures (moderate and hot) have been tested. Shape of the signal under the tire and magnitude of strain are compared with viscoelastic model pavement calculations.*

Introduction

Fatigue cracking and rutting are common pavement failures resulting from traffic loading and climate environment. One type of cracking is initiated at the bottom of the asphalt layer and propagates towards the surface (bottom-up cracks). Another type is initiated at or near the surface of the hot mix asphalt layers and propagates downward through the bound layers (top-down cracking). All these cracks can also propagate among interfaces between layers.To better understand these modes of failure, the knowledge of strain distribution through the asphalt layer is necessary. This paper is part of a collaborative project between Laval University (Québec, Canada) and the IFSTTAR (Nantes, France) with the main objective to characterize the strain occuring through the asphalt layers under several loading conditions. Two different tires, with various inflation pressures, four applied loads and two asphalt temperatures have been tested. Fiber optic strain sensors were installed at different depth of the pavement structure. The objectif of this paper is to contribute to a better understanding of the near-surface strains induced by dual tires in the asphalt layer. More specifically, the effect of asphalt temperature on the transverse and vertical strains is analysed. An asphalt layer at moderate temperature around 18°C and at hot temperature around 40°C has been tested. The discussion is based on experimental results and theorical solutions computed by the *ViscoRoute2.0©* software using a viscoelastic model[1].The paper includes a description of the pavement structure, the material properties and the sensors. The experimental results are presented and analysed in comparison with computed strain signals from the upper part of the first layer.

Experiment description

IFSTTAR's facility, pavement structure

The tests were conducted at the IFSTTAR's accelerated pavement testing facility [2]. The outdoor test track is a large scale circular track and a loading system with a mean radius of 19 m, a width of 3 m and a total length of 120 m. The device includes a central motor unit and four arms. Each arm lies on a module wich can be equipped with various load configurations. Each module can move during revolution around a mean position to simulate the lateral wandering of the traffic.
Two pavement sections, representing 1/3 of the whole test track, were built in February 2011 and instrumented in May 2011 . The two sections present different structure in terms of asphalt concrete thickness. The first structure A (figure 1) is 22 m long and it consists of the following layers: 70 mm bituminous wearing course (layer N°1), a 60 mm binder course (layer N°2), a 300 mm granular subbase (layer N°3) and a sandy subgrade soil (layer N°4). The second structure B (figure 2) is 18 m long and it includes only one 70 mm bituminous wearing course resting on a base and a subgrade soil similar to the first structure.

Material properties

Each layer of the structure is considered to be homogeneous and linear. The subbase is divided into three 100 mm-thick layers (layer N°3.1 to 3.3). The mechanical behaviour of the soil (layer N°4) and the unbound granular material are assumed to be elastic and the Poisson's ratio value is fixed to 0.35. With the help of elastic back calculations, their elastic modulus are supposed to be respectively E_4 = 80 MPa, $E_{3.3}$ = 160 MPa, $E_{3.2}$ = 320 Mpa and $E_{3.1}$ = 640 Mpa. The bituminous wearing course is an asphalt concrete 0/10 with 5.48% of 35/50 bitumen and 7% voids. The binder course is bituminous mix 0/14 with 4.49% of 35/50 bitumen and 9.6% voids. The mechanical behaviour of asphalt materials is modelled using the Huet-Sayegh model [3] [4]. The complex modulus is represented by five viscoelastic coefficients: E_0 (static elastic modulus), E_∞ (instantaneous elastic modulus), k and h (exponents of the parabolic dampers), δ (positive dimensionless coefficient) and three thermal coefficients A_0, A_1, A_2. At frequency ω and temperature θ, the complex modulus is Eqn (1):

$$E^*(\omega,\theta) = E_0 + \frac{E_\infty - E_0}{1+\delta\left(j\omega\tau(\theta)\right)^{-k}+\left(j\omega\tau(\theta)\right)^{-h}} \quad and \quad \tau(\theta) = \exp\left(A_0 + A_1\theta + A_2\theta^2\right) \quad (1)$$

According to French standards, complex modulus tests have been performed on the two bituminous materials. The software *Viscoanalyse* [5] was used to fit the laboratory data and calculate the eight parameters of the model. These values are shown in Table I. Poisson ratio ν is assumed to be equal to 0.32 at moderate temperature and equal to 0.38 at hot temperature for every asphalt material.

Table I: Huet-Sayegh parameters for bituminous materials

	E_0(MPa)	E_∞(MPa)	δ	k	h	A_0(t)	A_1(t °C^{-1})	A_3(t °C^{-1})
Layer 1	32	28 440	2.53	0.25	0.71	2.1688	-0.3671	0.00196
Layer 2	24	29 155	2.35	0.23	0.69	1.9706	-0.3670	0.00196

Sensors

Two innovative retrofit techniques which allow measuring strains in the upper and lower parts of the asphalt layer and also at the interface between two layers have been used on the two structures. These two technologies are: an asphalt concrete core specially trimmed for the installation of optic fiber gauges [6]; and a thin polymeric plate instrumented and fixed inside a saw cut in the asphalt layer [7]. Both systems use polymeric proof bodies selected to be mechanically (elastic modulus) and thermally (coeffficient of thermal expansion) compatible with asphalt concrete. The association of these two techniques allows obtaining the strains in three directions: longitudinal (ε_{xx}) transverse (ε_{yy}) and vertical (ε_{zz}).
Two optic fiber sensors are inserted into a polymeric proof body (gray area on figure 1 and figure 2) at orthogonal directions and fixed on the concrete core which allows measuring longitudinal and transverse strains. On the structure A, the sensors are first, positioned at the bottom of the first layer (figure 1-a) at Z=65 mm, then at the bottom of the second layer (figure 1-b) at Z=125 mm. On the structure B, the sensors are installed at the bottom of the layer (figure 2-b) at Z=65 mm and near the top (figure 2-a) at 10 mm.

The polymeric plates have been designed to be instrumented at various positions and installed in a saw cut perpendicular to the direction of travel. To evaluate the interface conditions between the asphalt layers of the structure A, ten horizontal sensors are placed on both sides of the interface. Five are at the bottom of the first plate (figure 1-c) at Z= 65 mm, and five at the top of the second plate (figure 1-d) at Z=75 mm. The first plate is also instrumented with five horizontal sensors at

Z=15 mm and five vertical sensors at Z=20 mm. Finally, five horizontal sensors are installed at the bottom of the second layer at Z=125 mm. On the structure B, the plate is instrumented with twenty one sensors (figure 2-c), seven horizontal sensors at Z=10 mm, seven vertical sensors at Z=20 mm and seven horizontal at Z=65 mm. All the plates are symmetrical, the sensors are spaced six centimeters and the central sensor is positioned directly under the center line (Y= 0 mm). Thermocouples are located at 48,38,23,12,9,6,3,0 cm depth inside the pavement.

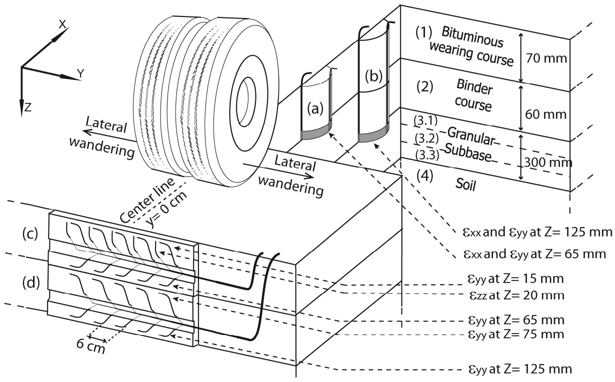

Figure 1: Configuration and instrumentation of the structure A (two instrumented concrete cores (a and b) and two instrumented polymeric plates (c and d))

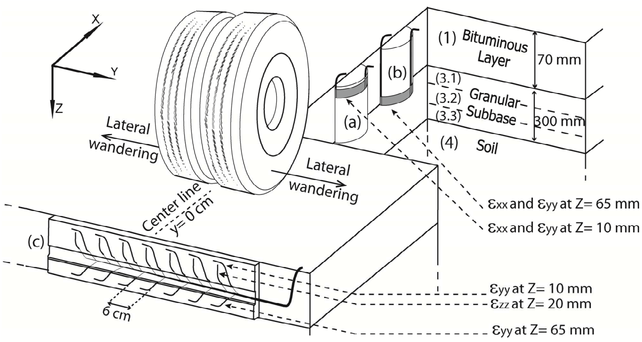

Figure 2: Configuration and instrumentation of the structure B (two instrumented concrete cores (a and b) and one instrumented polymeric plate (c))

Experimental protocol

The moving load is applied using a dual tire 12.00R20. The applied load (65 kN), the inflation pressure (850 kPa) and the revolution speed (6 rpm, which correspond to about 42km/h) were maintained during the whole experimental program. The data acquisition was performed at a 1 000 Hz sampling rate. The measurements were carried out for:

- eleven lateral tire positions (five on each side of the center line spaced by 10.5 cm) aim to determine the strain basin. As shown on figure 3, this protocol allows to obtain 55 measurement points for the structure A (5 sensors multiplied by 11 positions) and 77 points for structure B (7 sensors multiplied by 11 positions).

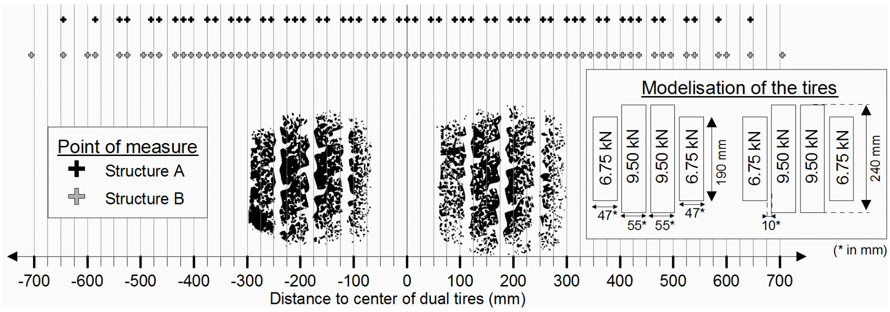

Figure 3: Distribution of measurement points under the footprint of the tire.

- two pavement temperatures. The tests took place on May 2011, allowing for moderate temperatures in the morning and hot in the afternoon. Table II summarizes the temperatures at different depths and their variation during tests.

Table II: Temperature at different depths of the tested pavements.

Temperature (°C)		surface	at 3 cm	at 6 cm	at 9 cm	at 12 cm
Structure A (25/05/2011)	Moderate	15.6° ± 2.6	17.1° ± 1.3	17.4° ± 0.7	18.6° ± 0.3	20.6° ± 0.2
	Hot	41.6° ± 0.9	42.4° ± 1.2	40.3° ± 1.0	37. 8° ± 0.5	33.6° ± 0.3
Structure B (24/05/2011)	Moderate	16.1° ± 0.8	18.6° ± 0.2	19.3° ± 0.3	20.8° ± 0.3	22.4° ± 0.3
	Hot	38.6° ± 3.2	38.2° ± 1.3	36.6° ± 1.1	34.9° ± 0.7	31.6° ± 0.1

Results and data analysis

Three dimensional strain occurring near the surface of structure B

For each gauge, an elementary data acquisition consisted in recording the signal during three rotations of the carousel allowing a verification of the repeatability of the signal. The dual tire moves in the X-direction. Thus, the signal which depends on time can be converted into a signal depending on spatial position X. Figure 4 presents typical responses of strain sensors that have been recorded near the surface, on structure B, under the right tire (in the plane y=100mm). The measured longitudinal, transverse and vertical strain are given for two temperatures. In these figures, contraction is represented by negative values of strains.
The following general observations can be made:

- The shape of longitudinal strains is not perfectly symmetrical. There is two zones of extension strains, one before the passage of the tire over the gauge (X positive) and the other after the passage (X negative). The magnitude of extension strain after the passage is the largest. The two magnitudes depend on the temperature. Due to the thermo-viscoelasticity of the material, the magnitude at higher temperatures is greater. The compressive strain zone is between both extension strain zones and it is associated with the passage of the load.

- The shape of transverse strains presents only a compressive zone. The magnitude of strain increases before the passage of the load to reach a peak under the tire and decreases slowly to zero.
- The vertical strains are extension at the front of the tire and decrease while the wheel is passing over. Despite the application of a vertical compressive stress caused by the wheel, the strain remains positive due to the Poisson's effect. After the load has passed, the strain reaches a second maximum and then decreases to zero. In contrast to the moderate temperature case, there is a contraction zone on the hot temperature curve, which occurs just in front of the tire. The signal reaches a negative peak, then decreases in two steps. The reduction is first rapid as the wheel leaves and then slower due to the relaxation of the material.

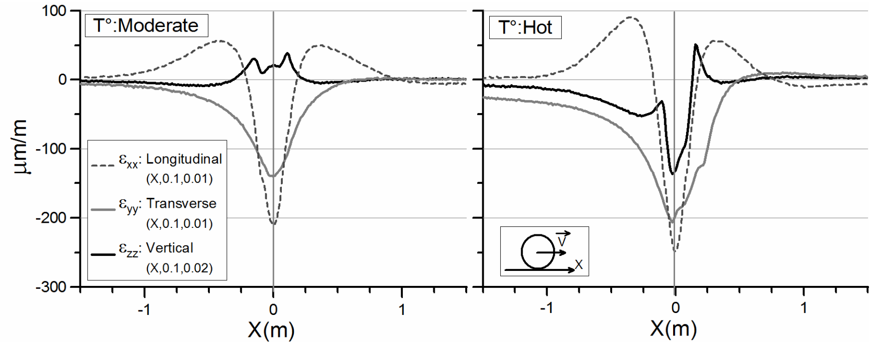

Figure 4: Strains near the surface for two temperatures (plan y=100 mm)

Modeling of the problem

A large number of transverse and vertical gauges were analysed and results denote a high sensitivity to the position under the passing load for both structure. Depending of the position under the tire, the signal presents different shapes and magnitudes. This variation can be induced by different stress states under the grooves and ribs of the tire. Under the tire, two characteristic curves have been identified and are presented in the next sections. In order to compare the measured strain signals, the software *ViscoRoute 2.0*© [1] has been used. In the software, the structure is represented by a multilayered half-space. This program integrates the viscoelastic behaviour of asphalt materials through the Huet-Sayegh model. The layers are assumed to be perfectly bonded (no slip). The influence of sliding interface condition on the response can be evaluated using the research version of *ViscoRoute* [8]. The load is assumed to move at a constant speed of 11.94 $m.s^{-1}$. The dual tire is discretized into eight rectangular shaped surfaces. Each rectangular load represents a tire tread as illustrated with the footprint on figure 3. Only a uniform vertical load is applied over the rectangular areas. To take account of the thermal gradient through the pavement, temperatures at 3 cm and 9 cm depth are used to model respectively the layer 1 and the layer 2.

Transverse strain occurring near the surface of structure A

For structure A, two types of signal shapes have been identified (figure 5):

- The shape N°1 for ε_{yy}(x,0.12,0.015) is the similar to the one previous illustrated on figure 4. The measured strain curves are showing time retardation and asymmetry that result from the viscoelastic properties of the material. The curves do not peak at X equals 0 but slightly after. The time delay is greater at higher pavement temperatures. Calculations did not result in the exact same shape as the measured strain curves and show more viscoelasticity and a wider zone of influence. The selected calculated curve was directly under a tire rib.
- The shape N°2 for ε_{yy}(x,-0.09,0.015) presents two peaks located at the front and the rear of the tire. The passage of the load imposes an inversion of the compressive strain curve. The maximum decrease is observed slightly after X equals 0. This time retardation is particularly pronounced at higher temperatures.

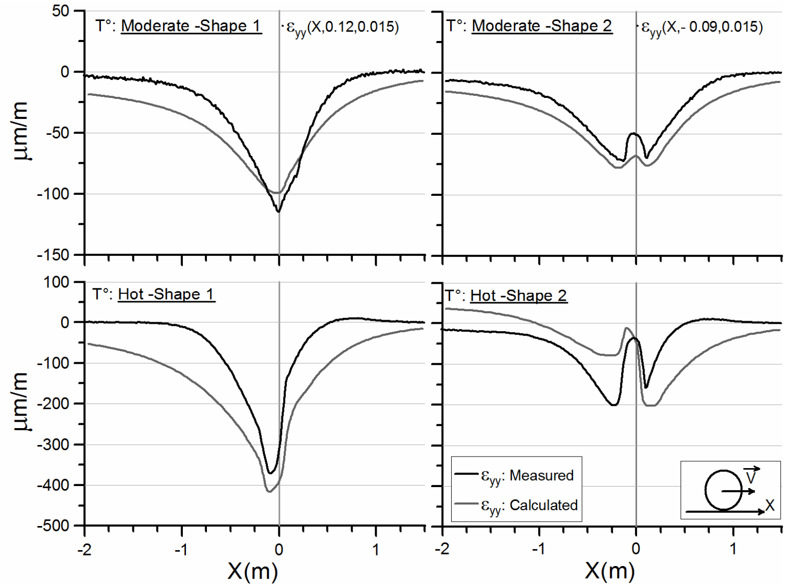

Figure 5: Transverse strain for two temperatures (structure A) at Z= 15 mm

Vertical strain occurring near the surface of structure A

For vertical strain, two shapes of the signal have been identified (figure 6):

- At moderate temperature, the curves present two peaks located before and after the passage of the wheel. Depending on the position under the tire, the vertical compressive stress can cause a significant decrease of the extension strain. The calculated strains have the same curve in the tensile zone preceding the passage of the tire. For the zone at the rear of the tire, the magnitude of calculated strains is lower. Nevertheless, the two curves are of similar order of magnitude.

- At hot temperature, the shape of the signal is the same as that described previously. Only the maximum magnitude in the compressive zone changes depending on the position under a groove (shape 1) or a rib (shape 2).The calculated strains in the tensile zone at the front of the tire are always higher than the measured ones.

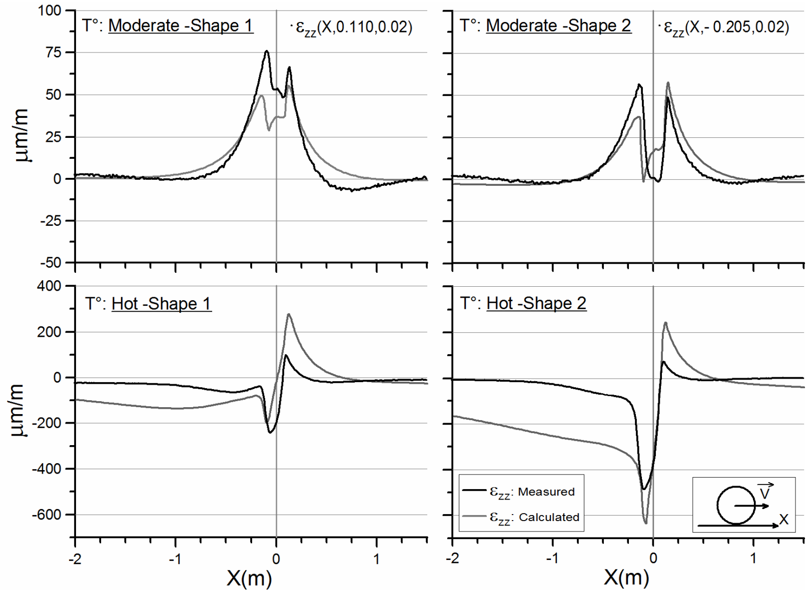

Figure 6: Vertical strain for two temperatures (structure A) at Z= 20 mm

Strain basin under the tire

All signals from transverse and vertical gauges were analysed and the value of the characteristic point near X= 0 mm was selected. Knowing the Y position under the tire, all the value are placed on the same graphic to form the strain basin (figure 7) and compared with the calculated curve. It can be observed that:

- For transverse strain: Away from the tire edges, the strains are positive indicating an extension strain. The measured values are higher than the calculated ones. At moderate temperature, the strain under the tire remains negative and experimental values are grouped. At hot temperature, the measured values are more dispersed due to the two possible shapes of curves. This dispersion is explained by the influence of grooves and ribs of the tire.
- For vertical strain: away from the tire edges and between dual tires, the strains are positive. The maximums are measured under the outside tires edges and between the two tires. This extension strain is a consequence of the Poisson's

ratio. The experimental values are lower than the calculated ones. Under the tire the measured and calculated values are of similar order of magnitude.

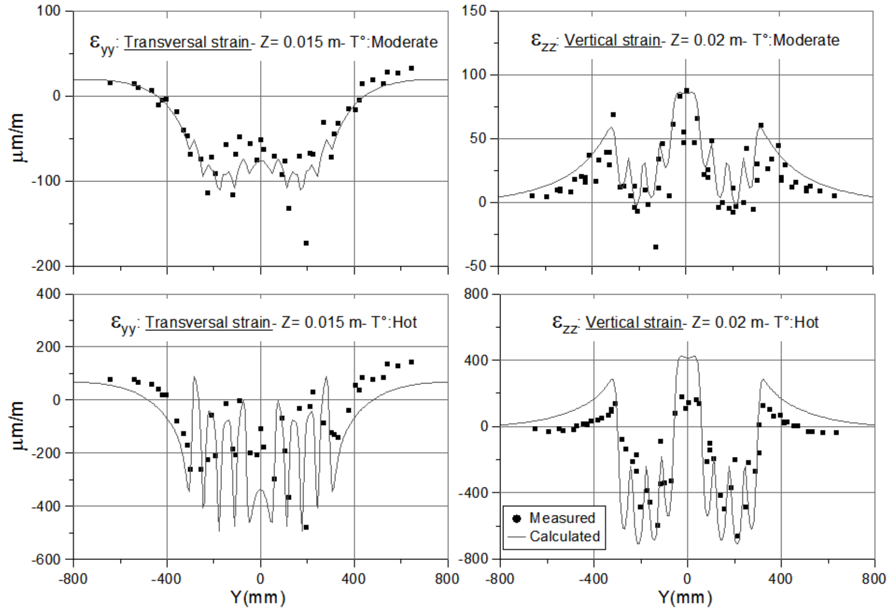

Figure 7: Measured and computed strain basins for two temperatures (structure A)

Discussion

The structure behaviour modeling computations were made with a constant uniform temperature for each layer. As shown on Table II, during measurements at moderate temperature, a negative temperature gradient was present in the layers 1 and 2. In contrast, the temperature gradient was positive at hot temperature. The stiffness differential in each asphalt layers has not been considered. Under each rib of a tire, three dimensional contact stresses are applied. In the modeling only a uniform vertical stress was considered. A more detailed load distribution with non-uniform transverse and longitudinal stresses could result in an even better fit. The two asphalt layers have been considered fully bonded together. Recent research indicates that debonding between asphalt layers increases shear stresses near the surface[9] [10]. The interface conditions are not the same between moderate temperature and hot temperature. The effect of interface bonding condition could be integrated into the model using the information obtained with the gauges installed on each side of the interface. The measured data are the average strains over the lengths of the gauges (10mm).Thus the recorded signal is not necessarily equal to the calculated strain at the same position under the tire. The presence of an aggregate near the sensor can increase the local modulus and modify the local visco-elasticity properties.

Conclusions

The use of optic fibre sensors positioned at two different depths within the asphalt concrete layer allowed to adequately characterize the strains occurring within this layer. The analysis of strain curves clearly demonstrated the differences existing between the two temperatures and the necessity to use a viscoelastic model. A detailed analysis of the strain basins revealed critical zones under or outside the tire. The same analysis will be done for all experimental conditions in order to evaluate the impact of each criterion on the pavement damage.

References:

[1] Chabot A., Chupin O., Deloffre L. and Duhamel D., (2010) ViscoRoute 2.0: a tool for the simulation of moving load effects on asphalt pavement *RMPD Special Issue on Recent Advances in Num. Simul. of Pavements,* 11 (2) pp 227-250.

[2] Hornych P., Kerzreho J.P., Chabot A., Bodin D., Balay J.M. and Deloffre L., (2008) The LCPC's ALT facility contribution to pavement cracking knowledge. In: *Pavement Cracking*, Proc. of the Sixth Internat. RILEM CP conference, Chicago, USA, pp 13-23, ISBN 978-0-415-47575-4.

[3] Huet C., (1963) Etude par une méthode d'impédance du comportement viscoélastique des matériaux hydrocarbonés. Ph.D dissertation, Université de Paris.

[4] Sayegh G., (1965) Contribution à l'étude des propriétés viscoélastiques des bitumes purs et des bétons bitumineux. Ph.D dissertation, Faculté Sciences de Paris

[5] Chailleux E., Ramond G., Such C., de la Roche C.(2006), A mathematical-based master-curve construction method applied to complex modulus of bituminous materials, *RMPDG*, Volume 7, pp. 75-92 EATA Special Issue.

[6] Doré G., Duplain G. and Pierre P., (2007) Monitoring mechanical response of in service pavements using retrofitted fiber optic sensors. In: Proc of the Intern. Conf. on the Advanced Charact. of Pavement and Soil Eng. Materials, Athens, Greece, pp 883-891, ISBN 978-0-415-44882-6.

[7] Grellet D., Doré G., and Bilodeau J.-P., (2010) Effect of tire type on strains occurring in asphalt concrete layers. In: Proc of the 11th Intern. Conf. On Asphalt Pavements, Nagoya, Japon.

[8] Chupin O., Chabot A., Piau J.-M., Duhamel D. (2010) Influence of sliding interfaces on the response of a layered viscoelastic medium under a moving load, In: *International Journal of Solids and Structures,* Volume 47, pp 3435-3446.

[9] Hammoum, F., Chabot, A., St-Laurent, D., Chollet, H., Vulturescu, B., (2010). Effects of accelerating and decelerating tramway loads on bituminous pavement. *Materials and Structures*, 43:1257–1269.

[10] Wang H., Al-Qadi I.L., (2010) Near-Surface Pavement Failure Under Multiaxial Stress State in Thick Asphalt Pavement. *Journal of the Transportation Research Board,* Volume 2154, pp 91-99.